Human Brain Mapping

WILEY

RESEARCH ARTICLE OPEN ACCESS

Changes in Functional Connectivity Relate to Modulation of Cognitive Control by Subthalamic Stimulation

Johannes Achtzehn[1,2] | Friederike Grospietsch[1] | Alexandra Horn[1] | Christopher Güttler[1] | Andreas Horn[1,3,4] | Ana Luísa de Almeida Marcelino[1,2] | Gregor Wenzel[1] | Gerd-Helge Schneider[5] | Wolf-Julian Neumann[1] | Andrea A. Kühn[1,6,7,8,9]

[1]Department of Neurology, Charité-Universitätsmedizin Berlin, Berlin, Germany | [2]Berlin Institute of Health (BIH), Berlin, Germany | [3]Center for Brain Circuit Therapeutics, Department of Neurology, Brigham & Women's Hospital, Boston, Massachusetts, USA | [4]Connectomic Neuromodulation Research at MGH Neurosurgery & Center for Neurotechnology and Neurorecovery (CNTR) at MGH Neurology, Massachusetts General Hospital, Boston, Massachusetts, USA | [5]Department of Neurosurgery, Charité-Universitätsmedizin Berlin, Berlin, Germany | [6]Bernstein Center for Computational Neuroscience, Humboldt-Universität, Berlin, Germany | [7]NeuroCure, Exzellenzcluster, Charité-Universitätsmedizin Berlin, Berlin, Germany | [8]DZNE – German Center for Neurodegenerative Diseases, Berlin, Germany | [9]Berlin School of Mind and Brain, Humboldt-Universität Zu Berlin, Berlin, Germany

Correspondence: Johannes Achtzehn (johannes.achtzehn@charite.de)

Received: 12 February 2024 | **Revised:** 13 November 2024 | **Accepted:** 24 November 2024

Associate Editor is co-author: Andreas Horn is a handling editor of *Human Brain Mapping* and a co-author of this article. To minimize bias, they were excluded from all editorial decision-making related to the acceptance of this article for publication

Funding: This study was supported by the Deutsche Forschungsgemeinschaft (DFG grant SPP2041, "Clinical connectomics: a network approach to deep brain stimulation" to A.A.K. as well as Emmy Noether Grant 410169619 to A.H.). The study was further funded by the Deutsche Forschungsgemeinschaft (DFG, German Research Foundation)—Project-ID 424778381—TRR 295 (to A.A.K., W.-J.N., and A.H.).

Keywords: cognitive control | deep brain stimulation | functional connectivity | Parkinson's disease | subthalamic nucleus

ABSTRACT

Subthalamic (STN) deep brain stimulation (DBS) in Parkinson's disease (PD) patients not only improves kinematic parameters of movement but also modulates cognitive control in the motor and non-motor domain, especially in situations of high conflict. The objective of this study was to investigate the relationship between DBS-induced changes in functional connectivity at rest and modulation of response- and movement inhibition by STN-DBS in a visuomotor task involving high conflict. During DBS ON and OFF conditions, we conducted a visuomotor task in 14 PD patients who previously underwent resting-state functional MRI (rs-fMRI) acquisitions DBS ON and OFF as part of a different study. In the task, participants had to move a cursor with a pen on a digital tablet either toward (automatic condition) or in the opposite direction (controlled condition) of a target. STN-DBS induced modulation of resting-state functional connectivity (RSFC) as a function of changes in behavior ON versus OFF DBS was estimated using link-wise network-based statistics. Behavioral results showed diminished reaction time adaptation and higher pen-to-target movement velocity under DBS. Reaction time reduction was associated with attenuated functional connectivity between cortical motor areas, basal ganglia, and thalamus. On the other hand, increased movement velocity ON DBS was associated with stronger pallido-thalamic connectivity. These findings suggest that decoupling of a motor cortico-basal ganglia network underlies impaired inhibitory control in PD patients undergoing subthalamic DBS and highlight the concept of functional network modulation through DBS.

Johannes Achtzehn and Friederike Grospietsch share first co-authorship.

1 | Introduction

Using cognitive control, humans can flexibly influence behavior based on set goals, which include overriding impulses by inhibiting responses in high conflict situations. The ability to adaptively withhold a response is important, as it allows an accumulation of evidence to increase decision accuracy at the price of reduced response speed. This conundrum is known as the speed-accuracy tradeoff (SAT) (Heitz 2014). The basal ganglia have been hypothesized as an integral part of a cortico-subcortical network that modulates motor inhibition (Jahanshahi et al. 2015). Within this network, the subthalamic nucleus (STN) is thought to modulate the decision threshold in conflicting situations and mediate motor inhibition (Aron et al. 2016; Bogacz et al. 2010; Herz et al. 2017; Zavala, Zaghloul, and Brown 2015) (for a recent review see Drummond and Chen 2020). Subthalamic deep brain stimulation (DBS), a standard treatment in Parkinson's disease (PD) (Deuschl et al. 2006), was shown to influence cognitive control and in particular, motor inhibition. In high decision conflict situations, which typically lead to a shift toward slower responses, STN-DBS lowers reaction times and inhibits an effective SAT (Frank et al. 2007; Ghahremani et al. 2018; Green et al. 2013; Hell et al. 2018; Herz et al. 2018) or in other words, increases motor impulsivity. For instance, when asked to decide whether a dot cloud moved left or right with varying difficulty levels, PD patients without STN-DBS slowed down their responses for more difficult choices (Herz et al. 2018). When STN-DBS was administered before the response was initiated, the ability to adapt reaction times to changing levels of difficulty diminished. In a recent study, Neumann et al. (2018) employed a visuomotor paradigm in which PD patients (both ON and OFF STN-DBS) and healthy controls were asked to move a cursor placed in the middle of a digital tablet either toward a target (automatic condition with congruent pen-to-target movement) or in the opposite direction of a target (controlled condition with conflicting pen-away-from-target movement). By measuring the reaction times in situations of low (automatic) and high (controlled) conflict, the impact of STN-DBS on motor inhibition could be investigated. Once the response is initiated, movement velocity, time, and error gave insights into kinematic aspects of motor control. The authors reported an impairment of response slowing for the (more difficult) controlled condition under DBS, which was dependent on the number of cortico-subthalamic fibers (i.e., hyperdirect pathway fibers) stimulated by STN-DBS. In terms of motor aspects of movement execution, STN-DBS increased movement velocity and error and decreased movement time. In a second step, a computational model of the cortex, basal ganglia and thalamus could predict the behavioral outcomes and suggested a differential effect of STN-DBS on the hyperdirect and indirect pathway.

Resting-state functional connectivity (RSFC), as estimated by correlations of ultra-low frequency blood oxygen dependent (BOLD) oscillations between different brain regions at rest, allows interrogation of polysynaptic pathway dynamics in relation to individual patient behavior. While Neumann et al. (2018) used normative tractography, our use of RSFC introduces significant advantages that enhance the scope of the investigation. Importantly, RSFC can reveal connectivity patterns that may not be evident through structural imaging alone, such as transient or flexible interactions between networks that are crucial for motor inhibition and thus, provides insights into the intrinsic functional organization of the brain. Furthermore, RSFC offers a subject-specific measure of brain connectivity, whereas normative tractography is based on population averages. By focusing on individual-level data, our approach accounts for variability in brain anatomy and connectivity, which is especially relevant when investigating the effects of DBS, as its outcomes can vary across patients depending on individual brain organization. This allows us to capture more nuanced changes in connectivity patterns that are associated with DBS and relate them more directly to motor inhibition. To this end, 14 PD patients received resting-state functional MRI (rs-fMRI) ON and OFF DBS and were tested on a separate day ON and OFF DBS in the same visuomotor task previously employed by Neumann et al. (2018). Given the evidence for a tight coupling between (fronto)-cortical and subcortical areas in inhibitory control (Alegre et al. 2013; Aron et al. 2016; Jahanshahi et al. 2015; Zavala et al. 2018; Zavala et al. 2014) and the correlation of reaction time slowing with hyperdirect pathway stimulation in Neumann et al. (2018), we hypothesized that STN-DBS induced changes in RSFC within cortico-subcortical connections related to motor preparation (i.e., reaction time). Because execution of movement is theorized to be less dependent on cortical input (Yttri and Dudman 2016), we hypothesized that STN-DBS-dependent changes in kinematic parameters may be accompanied by RSFC changes within the basal ganglia.

2 | Materials and Methods

2.1 | Behavioral Experiment and Kinematic Analysis

We included 14 right-handed PD patients (4 females, mean age 68 ± 6.56 years, for clinical details see Table S1) with STN-DBS. Ten of these patients were part of the cohort of a previous study (Horn, Wenzel et al. 2019) and had rs-fMRI data available, which were acquired 38.43 ± 30.42 months prior to the behavioral data (see Table S1). Four new patients were included and scanned with identical scan parameters. Exclusion criteria for the study included tremor in the dominant hand, severe head tremor in the DBS OFF state, severe psychiatric- or cognitive deficits, dementia (assessed with neuropsychological testing and psychiatric evaluation prior to surgery and deficient performance in the Montreal Cognitive Assessment score at the day of the experiment), and age of older than 80 years. All patients gave informed consent, and the study was approved by the local ethics committee (EA2/138/15) in accordance with the declaration of Helsinki.

The visuomotor task (Figure 1A) and set-up used in this study have been published previously and described in detail in de Almeida Marcelino et al. (2019) and Neumann et al. (2018). Briefly, participants used a pen on a tablet to steer a cursor on the screen in front of them and performed movements to move the cursor to a target appearing on the screen. Participants performed the task without resting their arm on any support to avoid obstruction of movement in all possible directions. The target

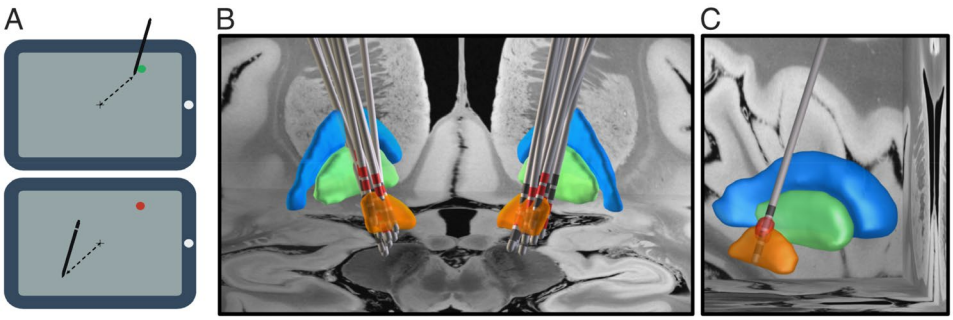

FIGURE 1 | (A) In the visuomotor task, patients either performed "automatic" movements with a pen following a cursor to hit a (green) target or performed inverted movements in a "conflicting" condition to hit a (red) target (pen-to-cursor mapping inverted). (B) DBS electrode localizations of PD patients. Active contacts (red) during bipolar stimulation in the STN (orange) are highlighted and superimposed on a section of the BigBrain ultrahigh resolution model (Amunts et al. 2013). (C) Stimulation of bipolar contacts of the electrode in the STN (orange) produces an oval-shaped volume of tissue activated (VTA).

was placed at one of eight random circular positions around the center. The task consisted of two behavioral conditions: in the automatic condition (green target), subjects moved the pen on the tablet in the direction of the target, that is, the pen-to-target mapping was congruent, while in the conflicting (controlled) condition (red target), subjects' movements had to be inverted, that is, to move the cursor toward the target they had to move the pen in the opposite direction (inverted pen-target mapping). Participants completed a total of 120 trials (60 trials for each condition) in blocks of 30 trials. The order of blocks was pseudorandomized over subjects and the condition of each block was announced at the beginning.

Patients performed the task twice, once in a bipolar stimulation mode that corresponded to the stimulation parameters active during the ON DBS fMRI scans, and once OFF DBS. The starting DBS condition was pseudorandomized. Since bipolar settings were used to conform with MRI safety guidelines, the stimulation amplitude was increased by up to 30% until motor symptoms disappeared (average stimulation amplitude in bipolar mode right: 3.39 ± 1.28 V; left: 3.65 ± 1.05 V, for stimulation details please see Table S2). Stimulation frequency and pulse width were not changed. Task performance was started at least 20 min after switching DBS to bipolar mode or switching DBS off. Patients were on their usual dopaminergic medication, as prescribed by their neurologist at the time of the behavioral task or rs-fMRI data acquisition and it was not changed for participation in the experiment. Minor adjustments in the medication regime between rs-fMRI acquisition and task performance was recorded for 5 out of the 14 patients.

2.2 | Analysis of Behavioral Data

The presented data correspond to mean ± SD and reported tests are randomized permutation tests (5000 permutations) judged at an alpha level of 0.05 (Winkler et al. 2014). Spearman's correlation coefficients were calculated throughout all correlation analyses if not specified otherwise. All measures tested or correlated were corrected for multiple comparisons by controlling for the false discovery rate (Benjamini, Krieger, and Yekutieli 2006). Where shown, the 95% confidence intervals were calculated in a nonparametric way by bootstrapping with 1000 samples (default values of the 'regplot' function, as part of the Python 'seaborn' package version 0.11.1). The 2.5th and 97.5th percentiles of the bootstrap distribution of the regression estimates are used as the lower and upper bounds of the confidence interval, respectively.

Analyses were carried out in MATLAB (The Mathworks, Natwick, MA) or with the SciPy (Virtanen et al. 2020) package in Python 3.8.

The first main outcome parameter of the task was reaction time (i.e., the time between target appearance and the first increase in movement acceleration in either of the two axes) and specifically, the difference in reaction time between automatic and conflicting trials that reflects the additional time associated with engagement of motor inhibition. By "motor inhibition," we refer to the ability to withhold a motor response in situations of high decision conflict (Aron 2007). This additional time is needed to accumulate and calculate evidence before initiating an adapted motor response for optimal behavioral performance. As the reaction time was defined as the time span from onset of target cue to the first movement of the pen, we hypothesize that a slower reaction time in conflicting trials reflects the time needed to engage motor inhibition, withhold the motor response and switch from an automatic (pen-to-target) to a controlled response (pen-away-from-target). Following the results of Neumann et al. (2018), the amount of slowing down should be affected by STN-DBS. Identical to Neumann et al. (2018), we compute the effect of STN-DBS on the percentage decrease in reaction time adaptation $\Delta RT_{STN-DBS}$ during conflicting trials as follows:

$$\Delta RT_{STN-DBS} = \frac{\Delta RT_{off}^{con.-aut.} - \Delta RT_{on}^{con.-aut.}}{\Delta RT_{off}^{con.-aut.}} \quad (1)$$

The variable $\Delta RT_{on}^{con.-aut.}$ reflects the average difference in reaction time (time from onset of the target to the first movement of the pen on the digital screen) between trials in the controlled condition and the automatic condition while DBS was OFF. Similarly, $\Delta RT_{on}^{con.-aut.}$ is derived by subtracting the reaction time of automatic trials from trials during the controlled condition during DBS. $\Delta RT_{STN-DBS}$ reflects the STN-DBS induced change in delay caused by the inversion

of pen-to-target mapping in conflicting trials and is robust against a potentially confounding effect of bradykinesia: patients who move slower might react slower, leading to greater absolute differences, regardless of the added cognitive load during conflicting trials.

The second main outcome parameter was movement velocity, which was obtained by taking the maximum of the first derivative of the movement trace:

$$v = \max\left(\frac{d\vec{s}}{dt}\right) \quad (2)$$

The values for the respective conditions (DBS ON vs. OFF, automatic vs. controlled) were calculated by averaging all trials within these conditions.

Additional parameters analyzed were movement time, calculated as the time difference between onset of movement and the cursor reaching the target, and trajectory error, computed as the mean difference between the cursor movement trace and the optimal path (i.e., a straight line) between source and target point.

2.3 | DBS Electrode Localizations and Modeling of VTA

All patients had bilateral DBS electrodes of the model 3389 Medtronic, Minneapolis, MN. Stimulation of the STN during task and rs-fMRI acquisition was done by the patients' implantable pulse generator (see Table S2 for details of stimulation parameters). Lead placement was confirmed with microelectrode recordings during surgery, intraoperative macrostimulation, and postoperative imaging. Pre- and postoperative imaging data was inspected for movement artifacts and approved by neuroradiologists. Using the pre- and postoperative imaging data, DBS electrodes were localized using the Lead-DBS toolbox following the enhanced default procedure of version 2.1.7 (www.lead-dbs.org) (Horn, Li et al. 2019) (Figure 1B). VTA volumes for the bipolar stimulation settings were simulated in native space using the SimBio/FieldTrip approach implemented in Lead-DBS for each hemisphere. Briefly, the static formulation of the Laplace equation is solved within a discretized domain using the finite element methods. Separate compartments for gray and white matter, metal and insulation material of the electrode were included in the tetrahedral mesh. Subsequently, the VTAs were transformed into MNI space and their relative overlap with the sensorimotor part of the STN (mSTN) or associative part of the STN (aSTN) was calculated by dividing the intersecting volume by the total volume of the respective part.

2.4 | Resting-State fMRI Data Acquisition

The scanning protocol in this study corresponds to the one published by Horn, Wenzel et al. (2019). Patients were scanned on Siemens Magnetom Aera 1.5 T MRI for not more than 30 min in total (as limited by the DBS device MRI conditional approval). Before each scan, it was ensured that the B1+ rms did not exceed the allowed 0.002 mT (in adherence to the magnetic resonance condition regulations of the Medtronic Activa CE-certificate). First, a T1 MP-RAGE anatomical scan was carried out ($1 \times 1 \times 1$ mm voxels, repetition time: 2200 ms, echo time: 2.63 ms). Then, an rs-fMRI scan (scan time: 9.42 min, 210 volumes, $3 \times 3 \times 3$ mm voxels, 24 slices with distance factor 30%, phase encoding: A ≫ P, repetition time: 2690 ms, echo time: 40 ms, field of view: 200 mm) was carried out ON (bipolar) DBS (Figure 1C). After the first rs-fMRI scan, patients were briefly taken out of the scanner and DBS was switched OFF. When symptoms reappeared (as judged by the supervising neurologist or neuroradiologist), the patient underwent the same rs-fMRI scan again OFF DBS. The time interval between the two scans never exceeded 10 min. One patient (first one scanned, patient 1) had a different repetition time in the MRI scans (3500 ms). Patient 10 had to prematurely leave the scanner OFF DBS due to discomfort and the scan was aborted after 133 (instead of 210) volumes during the OFF DBS condition scan.

2.5 | Estimating Cortico-Thalamic-Basal Ganglia Connectivity

Connectivity between cortex, thalamus, and basal ganglia was estimated within voxels defined by a network parcellation with seven bihemispheric regions of interest (ROIs) that were chosen based on their potential involvement in cognitive control of motor response: STN (Aron et al. 2016; Neumann et al. 2018), internal/external pallidum (GPi and GPe) (Sohn and Hallett 2004), striatum (Zandbelt et al. 2013), motor thalamus (VAn, VAp, VLd/VLv nuclei combined) (Li et al. 2008), motor and premotor cortices, supplementary motor area (SMA), and pre-SMA (Jahanshahi et al. 2015). The ROIs were defined based on atlases available in Lead-DBS (see Table S3 for details on atlas components used in the parcellation).

Preprocessing of anatomical and resting-state data was carried out using Lead-Connectome version 2.1.7 (see Horn and Blankenburg 2016; Horn et al. 2014 for an in-depth description of the pipeline). Briefly, T1w images were first corrected for intensity nonuniformity with ANT's N4BiasFieldcorrection v2.1.0 (Tustison et al. 2010) and spatial normalization to the MNI152NLin2009cAsym template space was performed using antsRegistration. BOLD time series were first detrended and head motion was corrected using SPM12 (Friston et al. 1995). Next, a band-pass filter ($0.009\,\text{Hz} < f < 0.08\,\text{Hz}$) was applied, and the data was smoothed with an isotropic Gaussian kernel (FWHM = 6 mm). As nuisance regressors for noise removal, six head motion parameters (x, y, z, yaw, pitch, roll) as well as mean signals of white matter and CSF were used. Finally, BOLD images were aligned to the T1w using linear boundary-based registration with 9 DOF, as implemented in FSL flirt. All code is publicly available (https://github.com/netstim/leaddbs/).

After preprocessing, we used the GraphVar toolbox version 2.03 (http://www.rfmri.org/GraphVar [Waller et al. 2018]) to estimate changes between the ON and OFF DBS correlation matrices as a function of the change in behavioral parameters (this is referred to as 'Raw matrix (link-wise) mass

univariate approach' in GraphVar). The first covariate included in this analysis was the relative decrease in reaction time between automatic and conflicting trials induced by stimulation $\Delta RT_{STN-DBS}$ (see Equation 1). As the second covariate, the difference in movement velocity DBS ON—DBS OFF was used after averaging over automatic and controlled trials. We focused specifically on the difference between task-specific DBS effects on reaction time versus movement velocity to differentiate DBS-induced changes in cognitive (i.e., motor inhibition) versus kinematic motor control. We included the variable *months between task and scan* as an additional nuisance covariate in the model to control for potential variance introduced by different timepoints of rs-fMRI acquisition and performance of the behavioral task.

First, based on the network parcellation described above, connectivity matrices for ON and OFF DBS were calculated using the partial correlation measure (Wang et al. 2016). Next, a general linear model was used to identify ON-OFF DBS differences in each network link that were explained by DBS-dependent behavioral differences. To estimate the significance of components, we compared the correlations against random networks generated in GraphVar ('random_shuffle' function) using the NBS approach (Zalesky, Fornito, and Bullmore 2010). With this approach, *p*-values were calculated for each component and FDR-corrected for the number of comparisons. Significance was defined at an alpha level of 5%.

2.6 | Data Availability

The DBS MRI datasets generated and analyzed during the current study are not publicly available because of data privacy regulations of patient data, but are available from the corresponding author upon reasonable request after approval of the local data protection office. Lead-DBS (http://www.lead-dbs.org) and GraphVar (http://www.rfmri.org/GraphVar) are openly available software.

3 | Results

On average, patients had a disease duration of 16 ± 4 years and were scanned on average 60 ± 25 months after DBS surgery (see Tables S1 and S2). All patients were scanned at a different time than they conducted the experimental task (months between scan and task: 38.43 ± 30.42, see Table S1), but stimulation parameters were identical, and levodopa equivalent doses (LEDD) did not significantly differ between occasions (LEDD at task assessment: 665.50 ± 349.12; LEDD at scan day: 730.15 ± 516.98; $p_{corr} = 0.72$).

Clinical motor signs were assessed using UPDRS-III at three timepoints: ON DBS with patients' usual stimulation settings (UPDRS ON DBS: 14.93 ± 7.37), ON DBS in bipolar mode (UPDRS bipolar DBS: 16.43 ± 7.44), and OFF DBS (UPDRS OFF DBS: 28.69 ± 9.62). All patients exhibited satisfactory symptom reduction through DBS in bipolar mode ($t_{13} = 8.78$, $p_{corr} < 0.001$, see Figure S1C). Electrodes were accurately placed (Figure 1B) with an average coverage of the bilateral sensorimotor STN by bipolar stimulation of $58.11\% \pm 21.76\%$.

Framewise displacement (head motion) during the rs-fMRI scans was found to be in a tolerable range for all runs and did not differ significantly between the DBS ON and OFF condition (0.233 ± 0.145 mm for the OFF condition, 0.315 ± 0.147 mm for the ON condition, $p_{corr} = 0.1$).

3.1 | Behavioral Results

Task performance ON and OFF DBS, regarding the outcome parameters reaction time, movement velocity, and movement time, confirmed previous findings of this task in PD patients ON and OFF STN-DBS (Neumann et al. 2018) in a completely independent sample of PD patients under bipolar DBS.

Reaction times were faster ON versus OFF DBS in automatic ($RT_{on}^{aut.} = 1.02 \pm 0.39$, $RT_{off}^{aut.} = 1.24 \pm 0.59$, $p_{corr} = 0.003$) and conflicting trials ($RT_{on}^{con.} = 1.33 \pm 0.64$, $RT_{off}^{con.} = 1.81 \pm 1.03$, $p_{corr} = 0.003$), and faster in automatic versus conflicting trials ON DBS ($v_{on} = 7.13 \pm 2.39$, $p_{corr} < 0.001$) and OFF DBS ($v_{off} = 5.54 \pm 2.57$, $p_{corr} < 0.001$). During stimulation (DBS ON), the difference in reaction time between automatic and conflicting trials was significantly lower than in the DBS OFF condition ($\Delta RT_{on}^{con.-aut.} = 0.33 \pm 0.32$, $\Delta RT_{off}^{con.-aut.} = 0.57 \pm 0.61$, $p_{corr} = 0.02$; Figure 2A). Similar results were obtained for movement velocity: movements were faster ON versus OFF DBS in automatic ($v_{on}^{aut.} = 7.97 \pm 2.68$, $v_{off}^{aut.} = 6.41 \pm 2.87$, $p_{corr} = 0.001$) and conflicting trials ($v_{on}^{con.} = 6.30 \pm 2.41$, $v_{off}^{con.} = 4.67 \pm 2.43$, $p_{corr} = 0.004$) and faster in automatic versus conflicting OFF ($v_{off}^{con.} = 4.67 \pm 2.43$, $v_{off}^{aut.} = 6.41 \pm 2.87$, $p_{corr} < 0.001$) and ON DBS ($v_{on}^{con.} = 6.30 \pm 2.41$, $v_{on}^{aut.} = 7.97 \pm 2.68$, $p_{corr} = 0.004$). However, there was no condition-specific modulation by DBS present for movement velocity ($\Delta v_{on}^{con.-aut.} = 2.03 \pm 1.37$, $\Delta v_{off}^{con.-aut.} = 1.813 \pm 1.31$, $p_{corr} = 0.43$; Figure 2B), that is, PD patients ON DBS moved faster in either condition compared to OFF DBS.

The clinical benefit as expressed by the change in UPDRS-III score (OFF-ON bipolar) correlated with average movement velocity (automatic trials: $r = 0.69$, $p_{corr} = 0.031$; conflicting trials: $r = 0.40$, $p_{corr} = 0.15$). There was no correlation of UPDRS-III change and reaction time difference between automatic and conflicting condition OFF-ON ($r = 0.21$, $p_{corr} = 0.34$). Furthermore, neither reaction time change nor average movement velocity were significantly correlated with average stimulation amplitude (left and right averaged; $r = 0.26$, $p_{corr} = 0.41$ and $r = -0.07$, $p_{corr} = 0.819$, respectively) or average LEDD (at scan and task day averaged; $r = -0.35$, $p = 0.33$ and $r = -0.38$, $p_{corr} = 0.32$, respectively).

3.2 | VTA Modeling Results

The effect of STN-DBS on the percentage decrease in reaction time adaptation $\Delta RT_{STN-DBS}$ (see Equation 1) correlated significantly with the amount of associative STN stimulated by the VTA (Pearson's $R = 0.742$, $p_{corr} = 0.018$; Spearman's rho $= 0.705$, $p_{corr} = 0.031$; see Figure 2C). In other words, the larger the volume of aSTN affected by electrical stimulation, the less patients were able to adapt (i.e., slow down) their response during conflicting trials. An increase in movement velocity during

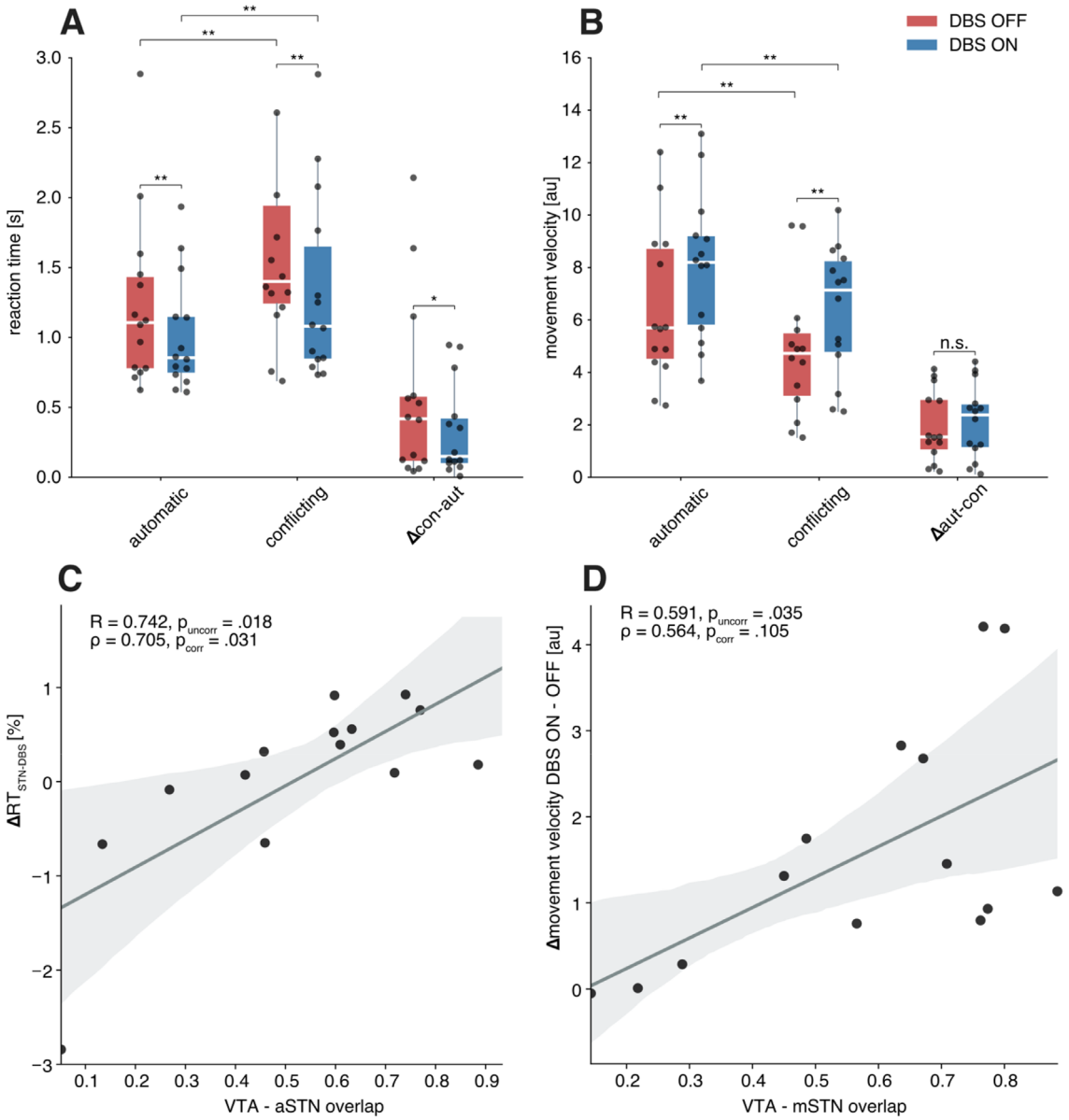

FIGURE 2 | Behavioral and VTA-STN overlap results. (A) Reaction time change under DBS differed by condition: ON STN-DBS, patients slowed down less for conflicting trials than OFF DBS, compared to the automatic condition. (B) Movements were faster ON than OFF DBS in both automatic and conflicting conditions and movements were faster in automatic than conflicting trials. (C) The amount of associative STN stimulated by the VTA correlated significantly with the effect of STN-DBS on the percentage decrease in reaction time adaptation (see Equation 1) and (D) the amount of sensorimotor STN stimulated correlated with the increase in movement velocity under STN-DBS. Upper and lower boundaries of the boxes represent 25% and 75%, respectively; whiskers extend to 1.5 time the interquartile range; $^{*}p < 0.05$; $^{**}p < 0.01$; n.s., not significant.

trials with STN-DBS ON correlated with the overlap of mSTN with the VTA, however the correlation did not remain significant after correcting for multiple comparisons (Pearson's $R = 0.591$, $p_{uncorr} = 0.025$, $p_{corr} = 0.075$; Spearman's rho = 0.564, $p_{uncorr} = 0.035$, $p_{corr} = 0.105$; see Figure 2D).

3.3 | Connectivity Analyses

Connectivity matrices ON and OFF DBS were compared against random networks using the GraphVar toolbox (Waller et al. 2018). Relative reaction time differences between automatic and controlled conditions were compared ON versus OFF DBS (see Equation 1) and correlated with connectivity change within the a priori defined parcellation. Two network regions were identified (Figure 3A) to show significant changes: first, a subnetwork of motor/premotor cortex and thalamus, GPi, and striatum and second, connectivity between STN and GPe (detailed correlation values are listed in Table S4). Functional connectivity between these nodes was significantly reduced by DBS the more patients exhibited a DBS modulation of cognitive motor control. In other words, the more patients' ability to slow down for conflicting trials (as compared to the automatic condition) was reduced under DBS, the less connected were motor/premotor cortex with (i) thalamus ($r = -0.693$; $p_{corr} = 0.025$), (ii) striatum ($r = -0.545$; $p_{corr} = 0.031$), and (iii) GPi ($r = -0.606$; $p_{corr} = 0.025$) and STN with GPe ($r = -0.49$; $p_{corr} = 0.048$).

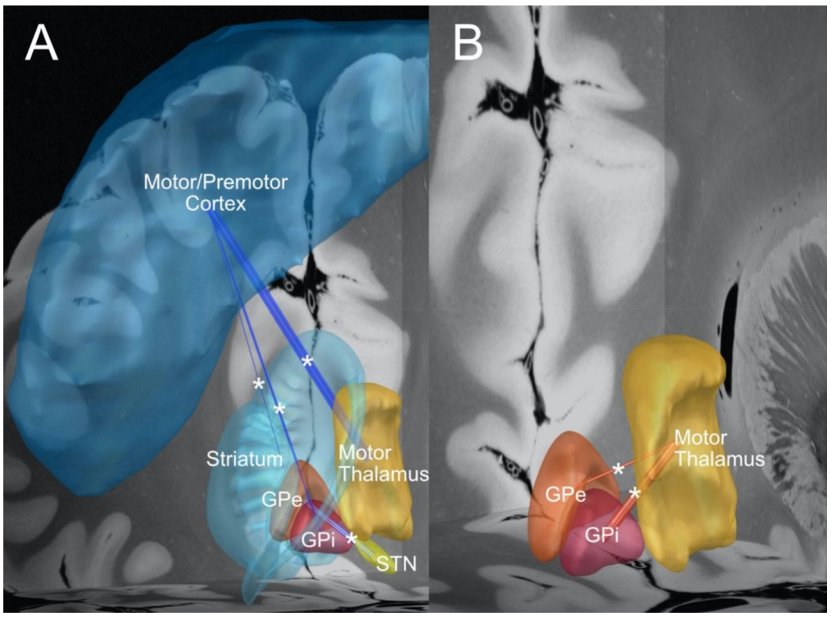

FIGURE 3 | Correlations between functional connectivity and behavior under DBS. (A) DBS-induced reduced response slowing in the conflicting condition correlated with a reduction of connectivity in a cortico-thalamic-basal ganglia network. In other words, the less patients are able to slow down reaction times during conflict, the less connected motor/premotor cortex is with (i) thalamus and (ii) parts of the basal ganglia and the less connected STN is with GPe. (B) Average movement velocity increased with DBS and this increase correlated with higher connectivity between thalamus and both pallidal segments. $*p < 0.05$; blue lines indicate reduction of functional connectivity; red lines indicate increase of functional connectivity. A schematic representation of these findings is shown in Figure S3 and the raw averaged connectivity matrices are presented in Figure S4.

In contrast, when connectivity change following DBS was correlated with average movement velocity across conditions ON-OFF, only one subnetwork was identified as a significant graph component, namely stronger connectivity between thalamus and GPi ($r = 0.577$, $p_{corr} = 0.01$) as well as thalamus and GPe ($r = 0.595$, $p_{corr} = 0.03$; Figure 3B). Otherwise stated, the higher the increase in movement velocity was in trials under STN-DBS, the stronger was thalamus became functionally connected to GPi and GPe.

4 | Discussion

In this study, we present novel mechanistic insights on how DBS-induced changes in RSFC influence inhibitory motor control in PD patients. We replicate behavioral results by Neumann et al. (2018), using the same task in a new patient sample with DBS in bipolar stimulation mode. The applied visuomotor task allowed assessment of kinematic parameters of movement (movement velocity) on the one hand, and parameters biased by motor inhibition (reaction time) on the other hand.

We report that STN stimulation modulated reaction time slowing based on engagement of motor inhibition: under DBS, patients slowed down less in the conflicting condition compared to the automatic condition than they did OFF DBS. A significant correlation between the volume of associative STN stimulated and reaction time slowing further corroborate the results and indicates an interference of STN-DBS with the engagement of cognitive inhibitory motor control, which normally facilitates an adaptation to higher task difficulties by delaying the response. As we used a relative measure of RT slowing, this effect is robust against the potential confound of improved bradykinesia during STN-DBS. Furthermore, no correlation was found between UPDRS-III and reaction time differences. The DBS-induced condition-specific modulation of reaction times was associated with a reduction of connectivity between motor and premotor cortex with thalamus, striatum and GPi as well as a reduced connectivity between STN and GPe. Thus, reduced inhibitory motor control induced by DBS in the conflicting condition was associated with a decoupling between cortex and basal ganglia-thalamic networks.

This effect was specifically related to reaction times and no condition-specific modulation by DBS was measurable for the kinematic parameter of movement velocity: while PD patients overall moved faster under DBS and faster in the automatic than the controlled condition, DBS did not interact with velocity differences between conditions. However, stronger pallido-thalamic connectivity was associated with faster movements ON versus OFF DBS. Like reaction time, the amount of sensorimotor STN stimulated correlated with the increase in movement velocity under DBS.

The results of this study should be carefully interpreted in the context of previous findings. The modulation of reaction times under DBS in situations that involve conflict or ambiguity between responses is well described (Ballanger et al. 2009; Cavanagh et al. 2011; Frank et al. 2007; Herz et al. 2018) and while the employed visuomotor task does not present patients with a high or low conflict reward choice, it does induce a visuomotor conflict in which participants have to switch from the easier automatic response (pen-to-target) to an inverted movement (pen-away-from-target) in the controlled condition. To increase reaction time and facilitate the change in response, motor inhibition must be engaged during the motor preparation

phase (time between cue onset and start of movement). In the current hypothesized model of motor inhibition, conflict is detected by the dorsomedial frontal cortex (pre-SMA), which recruits the STN via the hyperdirect pathway and thus, increases the inhibition of the thalamus and heightens the threshold for movement initiation (Zavala, Zaghloul, and Brown 2015). STN-DBS in PD could interfere with motor inhibition by suppressing local subthalamic firing (Milosevic et al. 2018), leading to an informational lesion (Grill, Snyder, and Miocinovic 2004). Consequently, a lack of comodulation of cortical input and thalamic output could lead to an interference of motor inhibition. More specifically, we demonstrate that subthalamo-pallidal coupling is reduced, which may hint toward a reduction of indirect pathway activity, which in turn may reduce pallidal control over thalamocortical activation. On a global BOLD level, this lack of synaptic control may lead to lower correlation of BOLD time series in key structures of cortex, basal ganglia, and thalamus, as both inhibition and excitation together may create fluctuations required for relevant coupling.

Alternatively, the reduction in reaction time adaption ON DBS may be interpreted in terms of enhanced inhibitory control, as patients became more proficient to resist the impulse to move the pen congruently toward the target in the controlled condition, allowing them to respond faster. While this interpretation cannot be ultimately ruled out with the empirical data of the current study, data from a previous study using the same paradigm and identical experimental conditions (Neumann et al. 2018) included healthy subjects as a control group. The study reported that healthy subjects and PD patients OFF DBS had similar reaction time adaptions while PD patients ON DBS had significantly less reaction time adaption (i.e., their reaction times were increased significantly less) during controlled trials. Considering the conceptualization of the STN as an integral part of action inhibition and DBS having the effect of an informational lesion, this indicates that STN-DBS introduced a pathological disruption of motor inhibition instead of enhancing inhibitory control.

Increased movement velocity under DBS, which was not influenced in a condition-specific manner by stimulation, was associated with stronger pallido-thalamic RSFC. This can be interpreted as a shift toward stronger subcortical modulation through suppression of subthalamic activity by DBS. Indeed, movement velocity in mice has been shown to be controlled by striatal stimulation of the direct and indirect pathway without altering cognitive functions such as action selection or motivation (Yttri and Dudman 2016). Furthermore, using recordings from magnetoencephalography, Oswal et al. (2016) reported that modulation on specifically the subcortical connections was correlated with parkinsonian symptom reduction, but not cortico-subthalamic coupling. In a computational basal ganglia model, a lesioning of the indirect pathway best explained an increase in movement time under STN-DBS in the same task as the present study (Neumann et al. 2018).

On average, participants ON DBS had a greater trajectory error than OFF DBS (see Figure S1). In contrast to results by Neumann et al. (2018), the differences were not significant. When compared to tasks in which trials have binary choices of varying conflict levels, this finding may seem surprising, as one would expect participants to have a higher error rate when their ability to adapt their reaction time is attenuated by STN-DBS. However, it is important to bear in mind that this visuomotor task was designed to segregate kinematic and inhibitory aspects of motor control. As trajectory error is calculated as the deviation of the movement trace from a straight line to the target, it is informative of the kinematic aspect of motor control after movement has been initiated. In contrast, we attribute the reduction of reaction time adaptation to the cognitive aspect of motor control during preparation of movement.

To control for a potential practice effect, we pseudorandomized the starting stimulation (DBS ON/OFF) and task (automatic/controlled) condition for all subjects, thus we do not expect to see an effect of learning over time in the averaged behavioral results. To further investigate this, we tested for a significant effect of task repetition by comparing reaction times between the two blocks within each combination of conditions. No significant effect of task repetition on reaction time was apparent (see Figure S2). Nevertheless, we cannot rule out any impact of potential practice effects, as previous studies have demonstrated that DBS can improve motor learning in the same task (de Almeida Marcelino et al. 2019).

While there was no significant correlation between changes in movement velocity and stimulation amplitude across patients, such a relationship was not tested on the individual level (i.e., only one stimulation setting was applied in each patient). We expect a lack of correlation to result from patient-to-patient variance in age, disease duration, and electrode placements.

Several limitations apply to the interpretation of this study's results. First, we would like to highlight that functional connectivity measured by BOLD fluctuations does not contain information about directionality or if connections are of mono- or polysynaptic nature. Furthermore, the given spatial resolution limits the ability to discern signals from structures in close proximity, such as the GPi and GPe due to the partial volume effect. To avoid a potential overinterpretation of the results, we consequently interpret our results on the more descriptive level of cortical-basal ganglia-thalamic loops (see Figure S3).

Second, the months between task and scan varied between patients, which could limit the interpretability of an association between behavior and connectivity. To regress out time between fMRI acquisition and task performance, we included this information as an additional covariate in our connectivity analyses. Importantly, all patients had an average disease duration of 16 years, DBS for a long time (60 months on average) and stimulation parameters and LEDD were stable between scan and task performance, indicating no significant changes of patients' clinical state.

Third, patients were tested ON their parkinsonian medication, which could have affected their behavior. However, dopaminergic drug intake did not correlate with the observed behavioral changes in this sample.

Finally, MR imaging in this specific study population could pose several problems. PD patients may move to a higher degree than healthy participants in the MR scanner, leading to movement artifacts. We prospectively excluded patients with severe

head tremor and calculated framewise displacements to assess movement in the scanner, which in all patients lay within an acceptable range. Furthermore, studies conducting rs-fMRI under DBS are still rare and advanced methodology and signal-processing steps are evolving. For example, new machine learning approaches to recover signal from areas that are affected by metal artifacts induced by DBS leads and subdermal wirings have been proposed (Yan et al. 2020). Ideally, these methods will be adopted in future studies after thorough validation. In the present study, we controlled for metal induced artifacts by using a coarse parcellation of the cortex, for example, including both motor and premotor cortex in one parcellation, and by averaging over both hemispheres for the connectivity analyses. Furthermore, we acknowledge that, even without DBS implants, signal-to-noise ratio is reduced within subcortical, iron-rich regions of the brain. However, safety regulations by the Medtronic Activa MR-conditional guidelines prohibited scanning at higher field strengths and limited the flexibility in fine-tuning scanning parameters, as suggested in for example de Hollander et al. (2017) and Miletic et al. (2020). Nonetheless, previous work, including 10 patients from the present study and using identical scanning parameters, provided evidence that BOLD time series from subcortical structures can be leveraged to gain insight into functional connectivity of cortico-subcortical networks, even in the presence of DBS metal artifacts (Horn, Wenzel et al. 2019).

Taken together, this study provides evidence for a DBS-induced decoupling within the cortical motor-basal ganglia network, leading to a reduction in inhibitory motor control in a visuomotor task. The results should be interpreted carefully with the limitations in mind and ideally be reproduced in a larger sample and without the time span in between scan and task performance. Understanding the connectivity basis of nonmotor changes in PD patients treated with DBS has a high clinical relevance, since network modulation may be fine-tuned with advancing therapeutic developments, such as adaptive stimulation.

Acknowledgments

We thank Johann Kruschwitz for his valuable input during the data analysis.

Conflicts of Interest

A.A.K. has received honoraria as speaker for Boston Scientific, Abbott, and Medtronic, all makers for DBS devices, which is not related to the current work. A.H. has received one-time speaker honoraria by Medtronic and Boston Scientific not related to the current work. The authors declare no conflicts of interest.

Data Availability Statement

The data that support the findings of this study are available on request from the corresponding author. The data are not publicly available due to privacy or ethical restrictions.

References

Alegre, M., J. Lopez-Azcarate, I. Obeso, et al. 2013. "The Subthalamic Nucleus is Involved in Successful Inhibition in the Stop-Signal Task: A Local Field Potential Study in Parkinson's Disease." *Experimental Neurology* 239: 1–12.

Amunts, K., C. Lepage, L. Borgeat, et al. 2013. "BigBrain: An Ultrahigh-Resolution 3D Human Brain Model." *Science* 340: 1472–1475.

Aron, A. R. 2007. "The Neural Basis of Inhibition in Cognitive Control." *Neuroscientist* 13: 214–228.

Aron, A. R., D. M. Herz, P. Brown, B. U. Forstmann, and K. Zaghloul. 2016. "Frontosubthalamic Circuits for Control of Action and Cognition." *Journal of Neuroscience* 36: 11489–11495.

Ballanger, B., T. van Eimeren, E. Moro, et al. 2009. "Stimulation of the Subthalamic Nucleus and Impulsivity: Release Your Horses." *Annals of Neurology* 66: 817–824.

Benjamini, Y., A. M. Krieger, and D. Yekutieli. 2006. "Adaptive Linear Step-Up Procedures That Control the False Discovery Rate." *Biometrika* 93: 491–507.

Bogacz, R., E. J. Wagenmakers, B. U. Forstmann, and S. Nieuwenhuis. 2010. "The Neural Basis of the Speed-Accuracy Tradeoff." *Trends in Neurosciences* 33: 10–16.

Cavanagh, J. F., T. V. Wiecki, M. X. Cohen, et al. 2011. "Subthalamic Nucleus Stimulation Reverses Mediofrontal Influence Over Decision Threshold." *Nature Neuroscience* 14: 1462–1467.

de Almeida Marcelino, A. L., A. Horn, P. Krause, A. A. Kuhn, and W. J. Neumann. 2019. "Subthalamic Neuromodulation Improves Short-Term Motor Learning in Parkinson's Disease." *Brain* 142: 2198–2206.

de Hollander, G., M. C. Keuken, W. van der Zwaag, B. U. Forstmann, and R. Trampel. 2017. "Comparing Functional MRI Protocols for Small, Iron-Rich Basal Ganglia Nuclei Such as the Subthalamic Nucleus at 7 T and 3 T." *Human Brain Mapping* 38: 3226–3248.

Deuschl, G., C. Schade-Brittinger, P. Krack, et al. 2006. "A Randomized Trial of Deep-Brain Stimulation for Parkinson's Disease." *New England Journal of Medicine* 355: 896–908.

Drummond, N. M., and R. Chen. 2020. "Deep Brain Stimulation and Recordings: Insights Into the Contributions of Subthalamic Nucleus in Cognition." *NeuroImage* 222: 117300.

Frank, M. J., J. Samanta, A. A. Moustafa, and S. J. Sherman. 2007. "Hold Your Horses: Impulsivity, Deep Brain Stimulation, and Medication in Parkinsonism." *Science* 318: 1309–1312.

Friston, K. J., J. Ashburner, C. D. Frith, J.-B. Poline, J. D. Heather, and R. S. J. Frackowiak. 1995. "Spatial Registration and Normalization of Images." *Human Brain Mapping* 3: 165–189.

Ghahremani, A., A. R. Aron, K. Udupa, et al. 2018. "Event-Related Deep Brain Stimulation of the Subthalamic Nucleus Affects Conflict Processing." *Annals of Neurology* 84: 515–526.

Green, N., R. Bogacz, J. Huebl, A. K. Beyer, A. A. Kuhn, and H. R. Heekeren. 2013. "Reduction of Influence of Task Difficulty on Perceptual Decision Making by STN Deep Brain Stimulation." *Current Biology* 23: 1681–1684.

Grill, W. M., A. N. Snyder, and S. Miocinovic. 2004. "Deep Brain Stimulation Creates an Informational Lesion of the Stimulated Nucleus." *Neuroreport* 15: 1137–1140.

Heitz, R. P. 2014. "The Speed-Accuracy Tradeoff: History, Physiology, Methodology, and Behavior." *Frontiers in Neuroscience* 8: 150.

Hell, F., P. C. J. Taylor, J. H. Mehrkens, and K. Botzel. 2018. "Subthalamic Stimulation, Oscillatory Activity and Connectivity Reveal Functional Role of STN and Network Mechanisms During Decision Making Under Conflict." *NeuroImage* 171: 222–233.

Herz, D. M., S. Little, D. J. Pedrosa, et al. 2018. "Mechanisms Underlying Decision-Making as Revealed by Deep-Brain Stimulation in Patients With Parkinson's Disease." *Current Biology* 28, no. 8: 1169–1178.e6.

Herz, D. M., H. Tan, J. S. Brittain, et al. 2017. "Distinct Mechanisms Mediate Speed-Accuracy Adjustments in Cortico-Subthalamic Networks." *eLife* 6: e21481.

Horn, A., and F. Blankenburg. 2016. "Toward a Standardized Structural-Functional Group Connectome in MNI Space." *NeuroImage* 124: 310–322.

Horn, A., N. Li, T. A. Dembek, et al. 2019. "Lead-DBS v2: Towards a Comprehensive Pipeline for Deep Brain Stimulation Imaging." *NeuroImage* 184: 293–316.

Horn, A., D. Ostwald, M. Reisert, and F. Blankenburg. 2014. "The Structural-Functional Connectome and the Default Mode Network of the Human Brain." *NeuroImage* 102, no. Pt 1: 142–151.

Horn, A., G. Wenzel, F. Irmen, et al. 2019. "Deep Brain Stimulation Induced Normalization of the Human Functional Connectome in Parkinson's Disease." *Brain* 142: 3129–3143.

Jahanshahi, M., I. Obeso, J. C. Rothwell, and J. A. Obeso. 2015. "A Fronto-Striato-Subthalamic-Pallidal Network for Goal-Directed and Habitual Inhibition." *Nature Reviews. Neuroscience* 16: 719–732.

Li, C. S., P. Yan, R. Sinha, and T. W. Lee. 2008. "Subcortical Processes of Motor Response Inhibition During a Stop Signal Task." *NeuroImage* 41: 1352–1363.

Miletic, S., P. L. Bazin, N. Weiskopf, W. van der Zwaag, B. U. Forstmann, and R. Trampel. 2020. "fMRI Protocol Optimization for Simultaneously Studying Small Subcortical and Cortical Areas at 7 T." *NeuroImage* 219: 116992.

Milosevic, L., S. K. Kalia, M. Hodaie, et al. 2018. "Neuronal Inhibition and Synaptic Plasticity of Basal Ganglia Neurons in Parkinson's Disease." *Brain* 141: 177–190.

Neumann, W. J., H. Schroll, A. L. de Almeida Marcelino, et al. 2018. "Functional Segregation of Basal Ganglia Pathways in Parkinson's Disease." *Brain* 141: 2655–2669.

Oswal, A., M. Beudel, L. Zrinzo, et al. 2016. "Deep Brain Stimulation Modulates Synchrony Within Spatially and Spectrally Distinct Resting State Networks in Parkinson's Disease." *Brain* 139: 1482–1496.

Sohn, Y. H., and M. Hallett. 2004. "Disturbed Surround Inhibition in Focal Hand Dystonia." *Annals of Neurology* 56: 595–599.

Tustison, N. J., B. B. Avants, P. A. Cook, et al. 2010. "N4ITK: Improved N3 Bias Correction." *IEEE Transactions on Medical Imaging* 29: 1310–1320.

Virtanen, P., R. Gommers, T. E. Oliphant, et al. 2020. "SciPy 1.0: Fundamental Algorithms for Scientific Computing in Python." *Nature Methods* 17: 261–272.

Waller, L., A. Brovkin, L. Dorfschmidt, D. Bzdok, H. Walter, and J. D. Kruschwitz. 2018. "GraphVar 2.0: A User-Friendly Toolbox for Machine Learning on Functional Connectivity Measures." *Journal of Neuroscience Methods* 308: 21–33.

Wang, Y., J. Kang, P. B. Kemmer, and Y. Guo. 2016. "An Efficient and Reliable Statistical Method for Estimating Functional Connectivity in Large Scale Brain Networks Using Partial Correlation." *Frontiers in Neuroscience* 10: 123.

Winkler, A. M., G. R. Ridgway, M. A. Webster, S. M. Smith, and T. E. Nichols. 2014. "Permutation Inference for the General Linear Model." *NeuroImage* 92: 381–397.

Yan, Y., L. Dahmani, J. Ren, et al. 2020. "Reconstructing Lost BOLD Signal in Individual Participants Using Deep Machine Learning." *Nature Communications* 11: 5046.

Yttri, E. A., and J. T. Dudman. 2016. "Opponent and Bidirectional Control of Movement Velocity in the Basal Ganglia." *Nature* 533: 402–406.

Zalesky, A., A. Fornito, and E. T. Bullmore. 2010. "Network-Based Statistic: Identifying Differences in Brain Networks." *NeuroImage* 53: 1197–1207.

Zandbelt, B. B., M. Bloemendaal, S. F. Neggers, R. S. Kahn, and M. Vink. 2013. "Expectations and Violations: Delineating the Neural Network of Proactive Inhibitory Control." *Human Brain Mapping* 34: 2015–2024.

Zavala, B., A. Jang, M. Trotta, C. I. Lungu, P. Brown, and K. A. Zaghloul. 2018. "Cognitive Control Involves Theta Power Within Trials and Beta Power Across Trials in the Prefrontal-Subthalamic Network." *Brain* 141: 3361–3376.

Zavala, B., K. Zaghloul, and P. Brown. 2015. "The Subthalamic Nucleus, Oscillations, and Conflict." *Movement Disorders* 30: 328–338.

Zavala, B. A., H. Tan, S. Little, et al. 2014. "Midline Frontal Cortex Low-Frequency Activity Drives Subthalamic Nucleus Oscillations During Conflict." *Journal of Neuroscience* 34: 7322–7333.

Supporting Information

Additional supporting information can be found online in the Supporting Information section.